

# Catalytic performance of Ni-Cu/Al<sub>2</sub>O<sub>3</sub> for effective syngas production by methanol steam reforming

Khzouz, M., Gkanas, E., Du, S. & Wood, J.

Author post-print (accepted) deposited by Coventry University's Repository

## Original citation & hyperlink:

Khzouz, M, Gkanas, E, Du, S & Wood, J 2018, 'Catalytic performance of Ni-Cu/Al<sub>2</sub>O<sub>3</sub> for effective syngas production by methanol steam reforming' *Fuel*, vol. 232, pp. 672–683.

<https://dx.doi.org/10.1016/j.fuel.2018.06.025>

DOI 10.1016/j.fuel.2018.06.025

ISSN 0016-2361

ESSN 1873-7153

Publisher: Elsevier

**NOTICE: this is the author's version of a work that was accepted for publication in *Fuel*. Changes resulting from the publishing process, such as peer review, editing, corrections, structural formatting, and other quality control mechanisms may not be reflected in this document. Changes may have been made to this work since it was submitted for publication. A definitive version was subsequently published in *Fuel*, [232], (2018)] DOI: 10.1016/j.fuel.2018.06.025**

© 2018, Elsevier. Licensed under the Creative Commons Attribution-NonCommercial-NoDerivatives 4.0 International

<http://creativecommons.org/licenses/by-nc-nd/4.0/>

Copyright © and Moral Rights are retained by the author(s) and/ or other copyright owners. A copy can be downloaded for personal non-commercial research or study, without prior permission or charge. This item cannot be reproduced or quoted extensively from without first obtaining permission in writing from the copyright holder(s). The content must not be changed in any way or sold commercially in any format or medium without the formal permission of the copyright holders.

This document is the author's post-print version, incorporating any revisions agreed during the peer-review process. Some differences between the published version and this version may remain and you are advised to consult the published version if you wish to cite from it.

1  
2  
3  
4  
5  
6  
7  
8  
9  
10  
11

# Catalytic Performance of Ni-Cu/Al<sub>2</sub>O<sub>3</sub> for Effective Syngas Production by Methanol Steam Reforming

Martin Khzouz<sup>1\*</sup>, Evangelos I. Gkanas<sup>1</sup>, Shangfeng Du<sup>2</sup>, Joe Wood<sup>3</sup>

1. *Hydrogen for Mobility Lab, Institute for Future Transport and Cities, Coventry University,  
Priory Street, Coventry CV1 5FB, United Kingdom.*

2. *School of Chemical Engineering, University of Birmingham, Edgbaston, Birmingham  
B152TT, UK*

3. *Catalysts and Reactions Group, School of Chemical Engineering, The University of  
Birmingham, Edgbaston B15 2TT, UK*

\*Email:ac2127@coventry.ac.uk

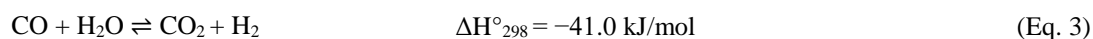
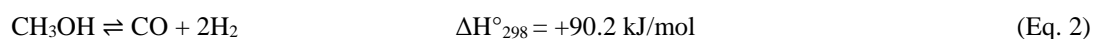
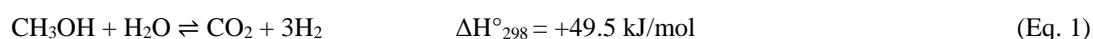
## Abstract

13 This work investigates the catalytic performance of bimetallic Ni-Cu/Al<sub>2</sub>O<sub>3</sub> catalysts for syngas  
14 production by methanol steam reforming. The synthesis and characterization of a series of Ni<sub>x</sub>-Cu<sub>y</sub>/Al<sub>2</sub>O<sub>3</sub>  
15 catalysts with various stoichiometric fractions (x= 10, 7, 5, 3 and 0wt% and y= 0, 3, 5, 7 and 10wt% to  
16 Al<sub>2</sub>O<sub>3</sub> support, respectively) are investigated and discussed. The catalytic performance is evaluated  
17 experimentally at temperature range of 225-325°C. Both mono-metallic catalyst (10wt.%Cu/Al<sub>2</sub>O<sub>3</sub> and  
18 10wt.%Ni/Al<sub>2</sub>O<sub>3</sub>) and bi-metallic catalysts (7wt.%Cu-3wt.%Ni/Al<sub>2</sub>O<sub>3</sub>, 5wt.%Cu-5wt.%Ni/Al<sub>2</sub>O<sub>3</sub> and  
19 3wt.%Cu-7wt.%Ni/Al<sub>2</sub>O<sub>3</sub>) are synthesized using an impregnation method and characterized by means of  
20 SEM, temperature programmed reduction (TPR), BET analysis, XRD and TGA. It is found that the  
21 bimetallic Ni-Cu catalyst had a strong influence on the amount of CO<sub>2</sub> and CO produced due to the  
22 different selectivity towards the water gas shift reaction and methanol decomposition reaction. The  
23 increase of the Ni content leads to an increase in CO and decrease in CO<sub>2</sub> yields. The bimetallic catalyst  
24 did not produce CH<sub>4</sub>, revealing that Cu alloying in Ni catalyst had an inhibiting effect for CO and/or CO<sub>2</sub>  
25 hydrogenation.

# 1. Introduction

Methanol is being used as source of fuel to produce syngas in small scale reformers [1]. The conversion of methanol to syngas takes place over a lower temperature range of 200-325°C compared to other liquid fuels such as ethanol which is only converted at temperatures above 500 °C. The absence of C-C bonds in methanol leading to low energy chemical bonds makes the reforming of methanol popular for the development of fuel processor for hydrogen production and electricity generation using fuel cells [2, 3].

The steam reforming of methanol (Eq. 1) ideally produces dry gases consisting of 75 vol% of hydrogen and 25 vol% carbon dioxide with complete stoichiometry conversion [4, 5]. The methanol steam reforming process (Eq. 1) [6-10] is represented by summation of decomposition reaction of methanol (Eq. 2) and water gas shift reaction (Eq. 3) [7, 11, 12]. According to the stoichiometry of the reactions, complete steam reforming of methanol notwithstanding equilibrium limitations is predicted using highly active and selective catalyst to produce hydrogen and carbon dioxide at a reforming temperature of (200-300°C) and at atmospheric pressure [7, 11, 12].



The bimetallic effect of catalyst for methane steam reforming was studied [13-15]. Ni-Cu based catalysts were discussed in the literature for steam reforming of both ethanol [16-18] and methanol [19-21]. Ni-Cu supported on carbon nanotubes have been studied recently [19] and it was observed that alloy Ni with Cu could weaken the adsorption between Ni and hydrogen thus enhancing the catalyst activity due to the increase of methanol contact with Ni particles.

Ni<sub>x</sub>Cu<sub>y</sub>-Al catalysts were also synthesised with different Ni-Cu contents [20]. The results showed that NiCu alloy had improved catalyst performance compared to the monometallic Cu for methanol and ethanol reforming. It was also demonstrated that the introduction of Cu in the catalyst formulation suppresses coke deposition and the sintering of the active phase in steam reforming. The addition of Cu revealed a positive effect by preventing the formation of methane with enhanced stability. The experiment was conducted by constant increase of the reaction temperature. However, it cannot prove

1 whether the formation of CH<sub>4</sub> from hydrogenation reaction was suppressed as the temperature was  
2 increasing during the experiment, for which a study under steady operation conditions was required.

3  
4 We also studied 5%Ni-5%Cu/Al<sub>2</sub>O<sub>3</sub> previously by comparison with two commercial catalysts:  
5 Ni/Al<sub>2</sub>O<sub>3</sub> and Cu/ZnO/Al<sub>2</sub>O<sub>3</sub>[21]. It was shown that Cu increased the active particle size of Ni compared  
6 to Ni/Al<sub>2</sub>O<sub>3</sub> and Ni improved Cu dispersion compared to Cu/ZnO/Al<sub>2</sub>O<sub>3</sub> catalyst. The bimetallic catalyst  
7 with 5%Ni-5%Cu/Al<sub>2</sub>O<sub>3</sub> proved to be very active both in methane and methanol steam reforming  
8 compared with commercial catalysts.

9 In the current work, we systematically investigated the bimetallic catalytic activity by performing  
10 reaction conditions for four hours in order to study the gas mixture composition under constant reaction  
11 temperature and stable operation conditions. The main problem that this work intends to answer is the  
12 effect of the metallic/alloy phase of the catalysts with different loadings on the catalytic performance  
13 towards syngas production. Thus, the reaction yields and pre and post characterisation of the catalysts  
14 are investigated for mono-metallic, bimetallic and physical mixture of single metal catalysts.

15 Various loadings of bimetallic, 7wt.%Cu-3wt.%Ni/Al<sub>2</sub>O<sub>3</sub>, 5wt.%Cu-5wt.%Ni/Al<sub>2</sub>O<sub>3</sub> and 7wt.%Ni-  
16 3wt.%Cu/Al<sub>2</sub>O<sub>3</sub> catalysts were synthesized using impregnation method and characterized by different  
17 techniques. The results were compared with the monometallic 10wt.%Cu/Al<sub>2</sub>O<sub>3</sub> and 10wt.%Ni/Al<sub>2</sub>O<sub>3</sub>  
18 catalysts.

## 20 **2.1 Catalyst preparation**

21 The Ni<sub>x</sub>-Cu<sub>y</sub>/Al<sub>2</sub>O<sub>3</sub> catalyst was synthesised via an impregnation method. Both mono-metallic  
22 catalysts, 10wt.%Cu/Al<sub>2</sub>O<sub>3</sub> and 10wt.%Ni/Al<sub>2</sub>O<sub>3</sub>, and bi-metallic catalysts (7wt.%Ni-3wt.%Cu/Al<sub>2</sub>O<sub>3</sub>,  
23 5wt.%Ni-5wt.%Cu/Al<sub>2</sub>O<sub>3</sub> and 3wt.%Ni-7wt.%Cu/Al<sub>2</sub>O<sub>3</sub>) were prepared. Nickel nitrate  
24 (Ni(NO<sub>3</sub>)<sub>2</sub>·6H<sub>2</sub>O) and/or copper nitrate (Cu(NO<sub>3</sub>)<sub>2</sub>·3H<sub>2</sub>O) provided commercially (Fisher Scientific)  
25 were dissolved in high purity ethanol (99.8%) using a magnetic stirrer. To ensure good mixing and  
26 dissolution, the mono-metal solution was mixed for 30 minutes. However, for the bi-metallic catalyst  
27 type, a copper metal solution was prepared by mixing the solution for 30 minutes, then nickel nitrate was  
28 added to the prepared solution and it was further mixed for 30 minutes. To the above-prepared nitrate  
29 metal solution, 6 grams of trilobe Al<sub>2</sub>O<sub>3</sub> supplied by Johnson Matthey were added and mixed for two

1 hours using an ultrasonic mixer/heating bath (Bandelin Sonorex bath) set at a temperature of 27°C. The  
2 catalyst was dried overnight in a static oven at 100°C. In the final preparation stage the catalyst was  
3 heated for calcination to 500°C at rate of 5°C/min, held at that temperature for 5 hours, then finally  
4 cooled at rate 5°C/min to ambient room temperature.

5 The prepared mono-metallic and bi-metallic catalysts in the rest of this work will be denoted as  
6 10%Cu, 10%Ni , 7%Ni-3%Cu, 5%Ni-5%Cu and 3%Ni-7%Cu for brevity.

## 8 **2.2 Catalyst characterization**

9 The catalysts were characterized using Scanning Electron Microscope (SEM), nitrogen  
10 adsorption-desorption cycles analysed by the Brunauer Emmett Teller (BET) method to determine  
11 surface area, Temperature Programmed Reduction (TPR), X-ray Diffraction (XRD) and Thermo  
12 Gravimetric Analyses (TGA).

13 A Philips XL-30 with LaB6 filament SEM fitted with an Oxford Instruments INCA Energy  
14 Dispersive X-ray Spectroscopy (EDS) system was used to study the catalyst morphology and  
15 composition for both fresh and spent catalysts. The SEM apparatus uses a NordlysS camera which is able  
16 to produce images with minimal geometric distortion at a resolution of 1344x1024 pixels. The SEM  
17 captures adjusted angle from 15°-130° upon a 50x50 mm stage. The scanned samples were coated with  
18 gold before being introduced to the microscope chamber. The external morphology of the samples was  
19 recorded in the range of 1 µm up to 100 µm and a two-dimensional image was displayed on the computer  
20 screen using INCA software.

21  
22 In order to determine the catalyst surface area and average pore size for fresh and spent catalysts,  
23 the samples were analysed by the nitrogen adsorption-desorption method. The measurements were  
24 carried out over approximately 1.4g of catalyst sample using a Micrometrics ASAP 2010 analyser.  
25 Accelerated Surface Area and Porosimetry (ASAP) use the static volumetric technique to determine  
26 surface area using N<sub>2</sub>physisorption isotherms at -196°C. The volume of gas adsorbed was recorded by  
27 the instrument. Then the experiment data collected was used to calculate the BET surface area and  
28 average pore size[22].

29

1 The TPR runs were conducted using a Micrometrics AutoChem 2920 Analyzer on 1g fresh  
2 catalyst ground by pestle and mortar. The catalyst sample was pretreated using argon as preparation gas  
3 at flow rate 50 ml/min for cleaning the entire lines of the apparatus. The sample was pretreated by  
4 increasing the temperature up to 500°C at 10°C/min and held for one hour in order to remove any  
5 moisture from the sample and tube, then the sample was cooled down to ambient temperature. After  
6 that, 10% H<sub>2</sub>/90% Ar at flow rate of 50 ml/min was introduced and the temperature was increased to  
7 900°C at 10°C/min to record hydrogen uptake using Thermal Conductivity Detector (TCD) [23].

8  
9 The XRD characterization was performed using a Bruker D8 Advanced Diffractometer. The  
10 catalyst was crushed using a mortar and pestle in order to obtain a powder of the catalyst then it was  
11 scanned and recorded at room temperature in the two theta range from 30° to 90°, with 0.02° step size  
12 and CuK $\alpha$  radiation,  $\lambda=0.154$  nm and  $K=0.9$ . The XRD patterns were assigned according to the XRD  
13 database (PDF-4+2012) provided by International Centre for Diffraction Data (ICDD).

14  
15 A TGA was carried out using a NETZSCH TG 209 F1 instrument [24]. The mass of the used  
16 catalyst was monitored against the programmed temperature in order to study the mass changes of carbon  
17 formed on the used catalyst [25]. The amount of carbon formation on the catalyst after the reaction for all  
18 operated catalysts at 225-325°C and S/C (steam to carbon ratio) of 1.7 was achieved by introducing air  
19 (50 ml/min) into 20 mg of the spent sample and heating the sample from 25°C to 900°C at a ramp rate  
20 of 10°C/min. Then, the catalyst selectivity for solid carbon ( $Sel_C$ ) was estimated as shown in Eq. 4.

$$Sel_C (\%) = 100 \times \frac{n_{carbon}}{n_{CH_3OH,in}} \quad (\text{Eq. 4})$$

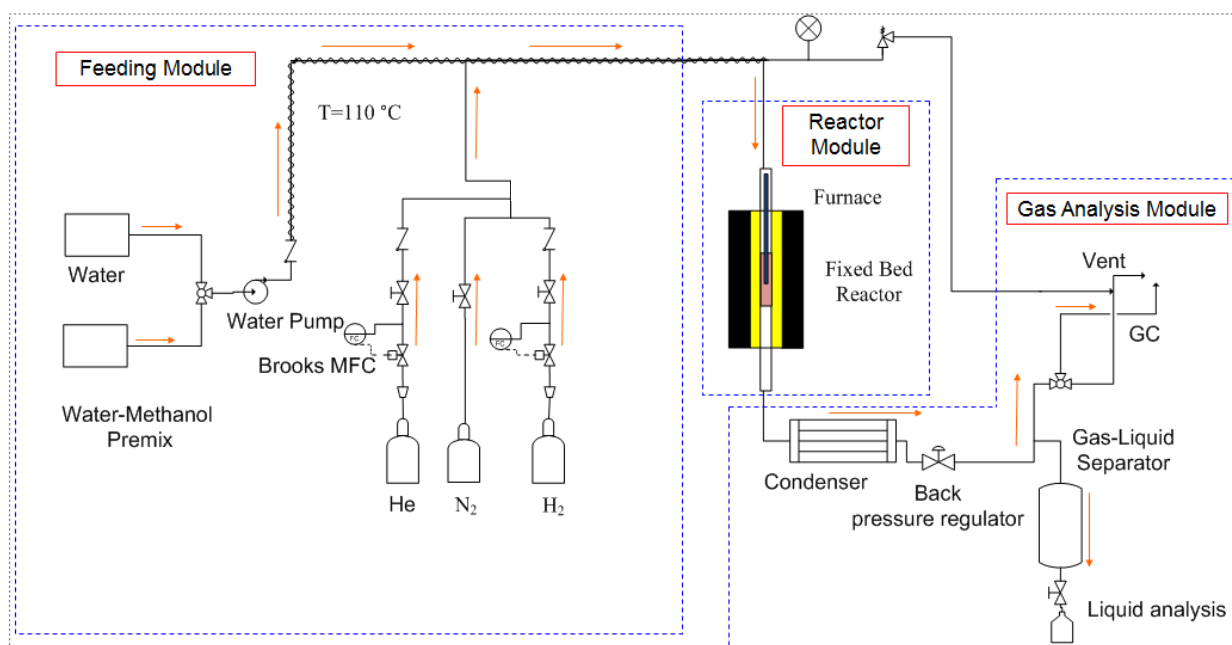
21  
22 Where  $n_i$  is total moles for reaction duration for species  $i$  (mol).

### 23 24 **2.3 Catalytic reactivity test**

25 The methanol steam reforming reaction was investigated in terms of reaction conditions, fuel  
26 conversion and the amount of H<sub>2</sub>, CO<sub>2</sub>, CO and CH<sub>4</sub> produced. Fig. 1 presents the experimental rig used  
27 for the current study. The rig consists of three modules; the feed, reactor and gas analysis modules. The  
28 feeding module is composed of a Cole-palmer EW-74930-05 series one pump which can supply water-

1 methanol premix to the vaporization zone and reactor. A vaporizer constructed from trace heating tape  
 2 (OMEGA FGR-100) wrapped around the feed pipe is used to generate steam at 110°C, the temperature  
 3 of which was controlled using a West 2300 PID controller. Digital Brooks mass flow controllers were  
 4 used to control the flow rate of the various gases fed to the reactor during the catalytic tests. The reactor  
 5 module consists of a high temperature furnace (Severn Thermal Solutions Ltd.). Inside the furnace, the  
 6 fixed bed reactor was constructed of stainless steel tube (316L) with inner diameter 10.9 mm, wall  
 7 thickness 0.89 mm and tube length of 395 mm. 3g catalyst was packed into the reactor and the void space  
 8 above and below was filled with glass beads; the catalyst bed height was 50mm. The temperature of the  
 9 reactor was measured using a K type thermocouple fixed near the centre of the bed. The reformat stream  
 10 at the outlet of the reactor was cooled before proceeding for gas analysis. Therefore, a condenser  
 11 facilitated by ice cubes in a bath surrounding a coiled section of the reactor outlet pipe at a temperature  
 12 of -2°C was used. After cooling, the unreacted liquid was separated from gaseous stream in a specially  
 13 designed gas-liquid separator unit. The various gases generated in the reaction were analysed using a  
 14 Refinery Gas Analyzer (RGA). The reformat gases were sampled using an online connection to Agilent  
 15 7890A model gas analyzer. The gas sample duration was five minutes before the generated gas was  
 16 withdrawn out to the vent.

17  
 18



19

20 Fig. 1. Experimental test rig flow sheet diagram.

1

2 Before the reaction commenced, the system was purged with N<sub>2</sub> for five minutes to remove the air  
3 from the pipes and reactor bed. Then, hydrogen at flow rate of 10 ml/min was introduced to reduce the  
4 catalyst at its reduction temperature determined from TPR (Fig.6), the TPR profile revealed that 10%Cu  
5 could be reduced at 250°C, 10%Ni at 650°C, 7%Cu-3%Ni at 350°C, 5%Cu-5%Ni at 380°C and 7%Ni-  
6 3%Cu at 425°C. The reduction process was carried out by raising the temperature to its target point at a  
7 rate of 5°C/min and maintaining it for 30 minutes in hydrogen flow before switching to pure N<sub>2</sub> for  
8 purging. Methanol steam reforming was carried out at temperatures of 225, 250, 275, 300 and 325°C in  
9 order to study the catalyst reactivity and methanol conversion. Distilled water mixed with pure methanol  
10 (99.99%) in a specific mole ratio of 1.7 was injected using the pump at constant flow rate of 0.06 ml/min.  
11 Then, the reactor was left for one hour in order for the temperature to stabilize under the reaction  
12 conditions. Once stable operation was achieved, samples were withdrawn for gas analysis, which was  
13 repeated every 15 minutes and recorded for 3 hours run duration of the catalyst reactivity test. The output  
14 flow rate was measured manually using bubble flow meter and stopwatch to calculate the flow rate of  
15 reformat.

16 In order to study conversions and products yields; an elemental analysis (carbon and hydrogen  
17 balance) using reactor exit concentrations of CO, CO<sub>2</sub>, CH<sub>4</sub> and H<sub>2</sub> and the inlet flow of methanol was  
18 performed. The unmeasured amount of H<sub>2</sub>O was calculated. The carbon balance Eq. 5 contains two  
19 unknowns,  $\dot{n}_{out,dry}$ ,  $\dot{n}_{CH_3OH,out}$ .

$$(y_{CO} + y_{CO_2} + y_{CH_4}) \times \dot{n}_{out,dry} + 1 \times \dot{n}_{CH_3OH,out} = 1 \times \dot{n}_{CH_3OH,in} \quad (\text{Eq. 5})$$

$y_i$  = mol fraction of species  $i$ .

$\dot{n}$  = total molar flow rate (mol / min)

$\dot{n}_i$  = molar flow rate of species  $i$  (mol / min)

20 where,  $in$  and  $out$  subscripts denote relevant mol entering or leaving the reaction.

21 The hydrogen balance analysis was performed as shown in Eq. 6. Hydrogen entering the  
22 reaction from water and methanol equals the hydrogen leaving the reaction. The Eq. 6 contains three  
23 unknowns,  $\dot{n}_{out,dry}$ ,  $\dot{n}_{H_2O,out}$  and  $\dot{n}_{CH_3OH,out}$



$$(2y_{H_2} + 4y_{CH_4}) \times \dot{n}_{out,dry} + 2 \times \dot{n}_{H_2O,out} + 4 \times \dot{n}_{CH_3OH,out} = 4 \times \dot{n}_{CH_3OH,in} + 2 \times \dot{n}_{H_2O,in} \quad (\text{Eq. 6})$$

$y_i = \text{mol fraction of species } i.$

$\dot{n} = \text{total molar flow rate (mol / min)}$

$\dot{n}_i = \text{molar flow rate of species } i \text{ (mol / min)}$

- 1 From the above elemental analysis, the unknown  $\dot{n}_{out,dry}$  was measured in the experiment from bubble
- 2 meter after water condensation,  $\dot{n}_{CH_3OH,out}$  and  $\dot{n}_{H_2O,out}$  were calculated.
- 3 The conversions for methanol and water were obtained by Eq.7-8:

$$x_{CH_3OH} = \frac{\dot{n}_{CH_3OH,in} - \dot{n}_{CH_3OH,out}}{\dot{n}_{CH_3OH,in}} \quad (\text{Eq. 7})$$

$$x_{H_2O} = \frac{\dot{n}_{H_2O,in} - \dot{n}_{H_2O,out}}{\dot{n}_{H_2O,in}} \quad (\text{Eq. 8})$$

- 4 The molar flow rates of products from the reaction were calculated by:

$$\dot{n}_{i,out} = y_i \times \dot{n}_{out,dry} \quad (\text{Eq. 9})$$

- 5 The products yields for hydrogen, carbon dioxide and carbon monoxide were obtained in mol/min per
- 6 mol/min of methanol as shown in Eq.10-12:

$$H_2 \text{ yield} = \frac{\dot{n}_{H_2,out}}{\dot{n}_{CH_3OH,in}} \quad (\text{Eq. 10})$$

$$CO_2 \text{ yield} = \frac{\dot{n}_{CO_2,out}}{\dot{n}_{CH_3OH,in}} \quad (\text{Eq. 11})$$

$$CO \text{ yield} = \frac{\dot{n}_{CO,out}}{\dot{n}_{CH_3OH,in}} \quad (\text{Eq. 12})$$

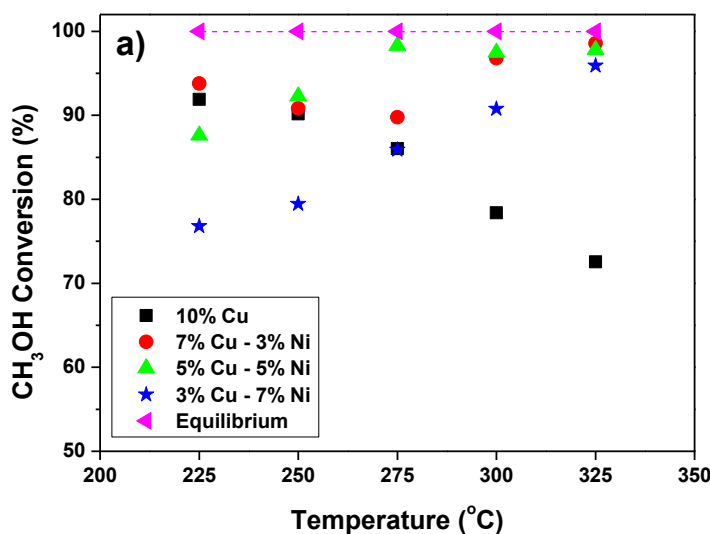
7

## 8 **3. Results and Discussion**

### 9 **3.1 Catalytic reactivity test**

1 The catalytic reactivity measurement was performed over a temperature range of 225-325°C, with  
 2 the S/C ratio of 1.7 and liquid hourly space velocity of 0.77h<sup>-1</sup>. The methanol and water conversions are  
 3 displayed in Fig. 2. The bimetallic catalyst revealed a lower water conversion than 10%Cu catalyst at all  
 4 operating temperatures and showed a superior methanol conversion at 300-325°C. For 7%Cu-3%Ni  
 5 catalyst, the methanol conversion decreased from 94% at 225°C to 90% at 275°C, then it showed an  
 6 increase up to 98.5% at 325°C. The 7%Cu-3%Ni catalyst revealed a slight increase in water conversion  
 7 within 225-275°C then it decreased rapidly within 300-325°C. The slight increase in water consumption  
 8 indicates that methanol steam reforming is a part of the reaction. However, the water consumption was  
 9 less than in 10%Cu catalyst for all temperatures which explains the existence of decomposition reaction  
 10 as explained later from the amount of CO produced. Both 5%Cu-5%Ni and 3%Cu-7%Ni catalysts  
 11 showed an increase in methanol conversion with increasing the reaction temperature (87.6%-97.8% for  
 12 5%Cu-5%Ni and 76.8-95.9% for 3%Cu-7%Ni) which is explained by the possible methanol  
 13 decomposition reaction that occurs on Ni species in bimetallic catalyst where a lot of CO was observed.  
 14 The water consumption for 5%Cu-5%Ni was less than 10%Cu and it decreased with increasing the  
 15 reaction temperature. There was no water consumption for 3%Cu-7%Ni, this explains the low methanol  
 16 conversion at low reaction temperature (225-250°C) since the methanol decomposition reaction is the  
 17 dominant and the conversion increase with increasing the reaction temperature.

18  
 19



20  
 21  
 22

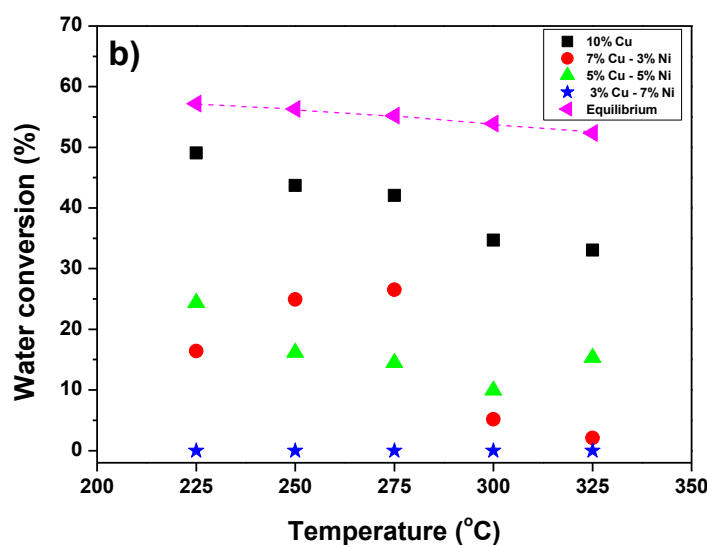
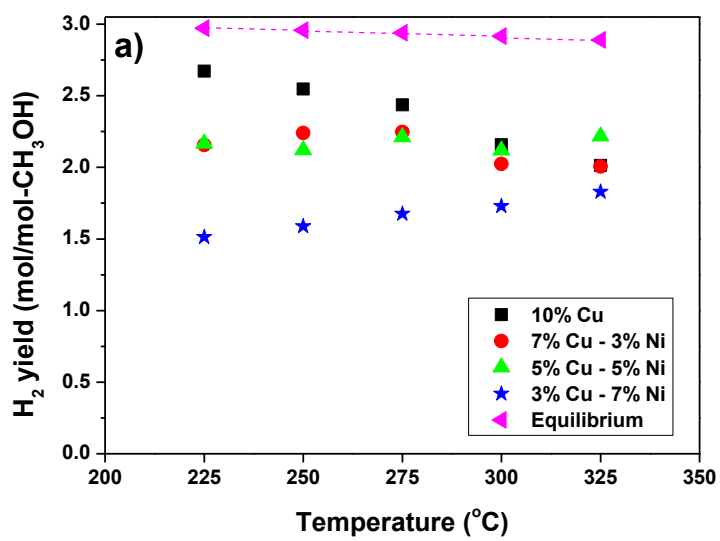


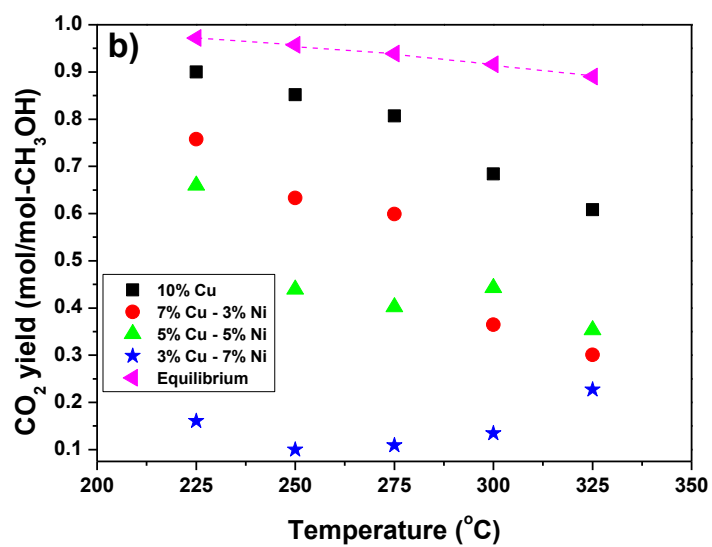
Fig. 2. Methanol and water conversion with S/C of 1.7 for 10%Cu, 7%Cu-3%Ni, 5%Cu-5%Ni and 3%Cu-7%Ni methanol catalysts: (a) methanol conversion and (b) water conversion

The steam reforming reaction showed that 10%Cu produced the highest amount of hydrogen within 225-300°C compared to other prepared catalysts, as shown in Fig. 3a. It was noticed that adding Ni metal to the Cu catalyst reduced the amount of hydrogen produced and showing that the bimetallic catalyst is less selective for hydrogen production than the monometallic Cu catalyst at such an operating temperature. The hydrogen yield of 2.2 mol/mol-CH<sub>3</sub>OH was observed for the 5%Cu-5%Ni catalyst at 325°C which is the highest amount for bimetallic catalyst at such temperature. The hydrogen yield was approximately constant (2.0-2.2 mol/mol-CH<sub>3</sub>OH) for 7%Cu-3%Ni and 5%Cu-5%Cu catalysts. The hydrogen yield increased from 1.5 mol/mol-CH<sub>3</sub>OH at 225°C to 1.8 mol/mol-CH<sub>3</sub>OH at 325°C for 3%Cu-7%Ni catalyst. More Ni metal in the catalyst made the catalyst less selective to hydrogen as observed for the 3%Cu-7%Ni catalyst. This confirms that Ni rich catalysts (with more than 5wt.%) are favourable for the decomposition reaction rather than the steam reforming reaction itself. For bimetallic catalyst, the decrease in hydrogen amount compared to 10%Cu could be due to the active methanol decomposition reaction over Ni and the reverse water gas shift reaction affecting the concentration of hydrogen produced as both reactions are thermodynamically favoured at such operation temperature.



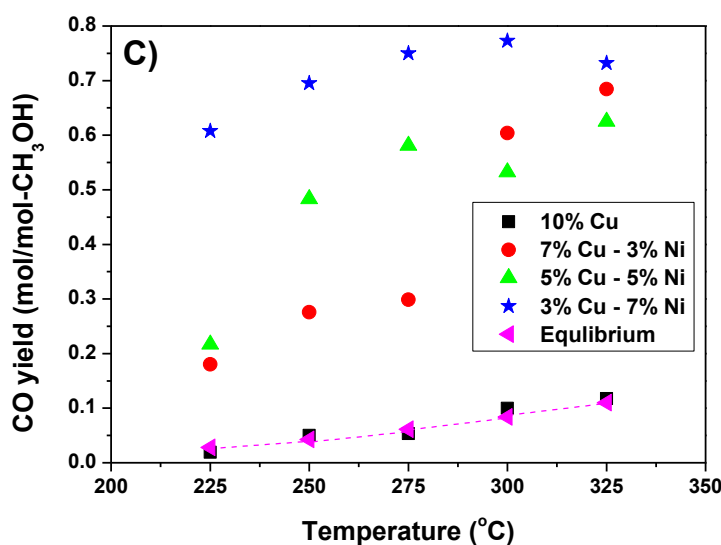
1

2



3

4



1

2 Fig. 3. H<sub>2</sub>, CO<sub>2</sub> and CO yields within 225-325°C and S/C of 1.7 for 10%Cu, 7%Cu-3%Ni, 5%Cu-5%Ni and 3%Cu-  
3 7%Ni methanol catalysts: a) H<sub>2</sub> yield, b) CO<sub>2</sub> yield and c) CO yield.

4 The carbon oxide yield profiles are presented in Fig. 3b and c as a function of temperature for various  
5 catalysts. The influence of increase the Ni content in the catalyst on reformat yield had shown an  
6 increase in CO and decrease in CO<sub>2</sub>. It is observed from Fig. 3b that increasing the amount of Ni content  
7 in the catalyst affects in a negative way for CO<sub>2</sub> production compared to 10% Cu. The amount of CO<sub>2</sub>  
8 formed in operated bimetallic catalyst is less than the amount obtained with the monometallic Cu catalyst.  
9 It was also observed that with 10%Cu, 7%Cu-3%Ni, 5%Cu-5%Ni catalysts, the amount of CO<sub>2</sub> decreased  
10 when increasing the temperature in the range of 225-325°C. However, the amount of CO<sub>2</sub> formed with  
11 3%Cu-7%Ni decreased within 225-275°C and then increased within 300-325°C, this observation is  
12 discussed later. From Fig. 3c, the amount of CO produced increased with the increase of Ni content upon  
13 the catalyst. The trend in CO yield with catalyst type is opposite to the trend of CO<sub>2</sub> shown in Fig. 3b.

14 In order to understand the effect of the Ni content, methanol steam reforming over 10% Ni catalyst  
15 was tested. The main products over 10% Ni (Table 1) were CO and H<sub>2</sub>, which were produced from the  
16 methanol decomposition reaction. The formation of a small amount of CO<sub>2</sub> is related to the water gas  
17 shift reaction. The methanol steam reforming over 10%Ni produced a significant amount of CH<sub>4</sub> due to  
18 CO and CO<sub>2</sub> hydrogenation which was not observed in 10%Cu and bimetallic Ni-Cu catalysts. The  
19 difference between 10%Ni catalyst and 10%Cu catalyst is that the latter one promotes the water gas shift  
20 reaction as observed from the formation of large quantities of CO<sub>2</sub> and small quantities of CO in Fig. 3b

1 and c, respectively. As a result, the water gas shift reaction equilibrium shifts towards the reactants with  
 2 increasing the temperature at which the conversion of CO to CO<sub>2</sub> is decreased as observed for 10% Cu  
 3 in Fig. 3b.

4 The bimetallic effect for Ni-Cu catalyst was also compared with the physical mixture of single metal  
 5 10%Cu and 10% Ni catalysts (Table 1). The reaction over the physical mixture of single metal 10%Ni  
 6 and 10% Cu (Table 1) showed significant formation of CH<sub>4</sub> which was not observed for 10% Cu and Ni-  
 7 Cu catalysts. Copper-based catalysts have good activity for the water gas shift reaction, and have no  
 8 methanation activity. The existence of single Ni catalyst in the reactor promotes CH<sub>4</sub> formation by CO  
 9 and CO<sub>2</sub> hydrogenation. The reaction over physical mixture of catalyst showed less CO and more CO<sub>2</sub>  
 10 than the bimetallic catalytic system. This indicates that the 10%Cu catalyst in the physical mixture of  
 11 catalyst controls the high activity of the water gas shift reaction.

12 *Table 1. Product yield for methanol reaction for 10%Ni and for physical mixture of single metal 10%Cu and 10%Ni*  
 13 *catalysts.*

14 \*Physical mixture of single metal (1.5 g of 10%Cu and 1.5 g of 10%Ni).

	Temperature (°C)	Conversion (%)		Yield (mol/mol CH <sub>3</sub> OH)			
		CH <sub>3</sub> OH	H <sub>2</sub> O	H <sub>2</sub>	CO <sub>2</sub>	CO	CH <sub>4</sub>
10%Ni	325	70.9	15.0	1.47	0.11	0.50	0.10
10%Ni, 10%Cu*	325	96.1	22.5	2.08	0.71	0.13	0.11
10%Ni, 10%Cu*	300	91.6	15.3	1.84	0.68	0.14	0.09
10%Ni, 10%Cu*	275	86.9	27.0	2.03	0.72	0.11	0.03

15

16 By comparing the carbon oxide yield over monometallic 10%Cu, 10%Ni and physical mixture of  
 17 single metals 10%Cu and 10%Ni catalysts, it was observed that the CO amount is strongly dependent on  
 18 the Cu content in the bimetallic Ni-Cu catalysts, which affects the water gas shift reaction equilibrium.  
 19 The decrease in Cu content with respect to Ni in the catalyst showed an increase in CO formation,  
 20 suggesting that the water gas shift reaction moves towards reactants. The increase in Ni content with  
 21 respect to Cu on the bimetallic catalyst revealed additional CO derived from the methanol decomposition  
 22 reaction. The bimetallic Ni-Cu catalyst did not produce CH<sub>4</sub>, suggesting an inhibiting effect of Cu  
 23 alloying for CO and CO<sub>2</sub> hydrogenation on Ni. Hence, that Cu has a low CO dissociation activity where

1 CO remains on the catalyst surface. As a result, the Cu presented in Ni-Cu catalyst prevents the CO  
2 activation on Ni sites in Ni-Cu catalyst.

3 The reaction activity profile (Fig. 3b and Fig. 3c) for carbon oxide yield for 3%Cu-7%Ni revealed  
4 slightly different trends over 5%Ni-5%Cu and 7%Cu-3%Ni catalysts. The amount of CO<sub>2</sub> formed with  
5 3%Cu-7%Ni decreased within 225-275°C then increased at temperatures in the range of 300-325°C. The  
6 Cu promotes the water gas shift reaction at low temperature and the reaction equilibrium moves towards  
7 the reactants by increasing the temperature. Hence, the CO amount will increase. On the other hand, Ni  
8 promotes methanol decomposition reaction and the reaction becomes very operative with increasing the  
9 temperature. Accordingly, it is expected that the amount of CO would increase and CO<sub>2</sub> decrease with  
10 increasing the reaction temperature as observed for 5%Ni-5%Cu and 7%Cu-3%Ni catalysts. Indeed, the  
11 reverse water gas shift reaction was found to be active at temperatures of 300-325°C for 7%Cu-3%Ni  
12 and 5%Cu-5%Ni catalysts, evidenced by a drop in water consumption (Fig. 2b.) at these high  
13 temperatures. For 3%Cu-7%Ni catalyst, the Ni rich alloy effect was observed. The Ni-Cu alloy phase is  
14 responsible for balancing the amount of CO with respect to CO<sub>2</sub>.

15 In summary, a higher metal content of Ni over Cu has a strong influence upon the amount of CO<sub>2</sub>  
16 by controlling the dominant reaction paths. When increasing the amount of Ni, the effect of bimetallic  
17 Ni-Cu becomes dominant in the reaction. The decomposition reaction on the metallic phase of Ni-Cu is  
18 responsible for producing a high amount of CO in the products. From the above results, the  
19 decomposition reaction of methanol occurs predominantly on the metallic phase of Ni-Cu and the reverse  
20 water gas shift reaction occurs at the Cu site and increase with increasing the reaction temperature, where  
21 these reactions are the major contributors for the CO production. The decomposition reaction mainly  
22 transforms methanol to CO and H<sub>2</sub> (Eq.2) and slow water gas shift reaction converts CO to CO<sub>2</sub> (Eq.3),  
23 the existence of the alloy phase of metal and/or metal phase determines CO<sub>2</sub> and CO amount. The  
24 increasing Ni metals content had a positive effect on methanol conversion and showed a high methanol  
25 conversion at 300-325°C. The methanol conversion was high for 5%Cu-5%Ni and 7%Cu-3%Ni (98.5%)  
26 at 325°C which could possibly be explained by the active decomposition reaction. The increase of Ni  
27 metals content showed an adverse effect on the amount of hydrogen produced. Increasing the amount of  
28 Ni metals content from 3% to 7% led to a big decrease for CO<sub>2</sub> and an increase for CO. It is also noticed  
29 that the bimetallic Ni-Cu catalyst produced negligible amount of CH<sub>4</sub>. It was validated experimentally

1 in this work that performing methanol steam reforming reaction over pure 10%Ni catalyst or over  
2 physical mixture of single metal 10%Ni and 10%Cu catalysts at 325°C and S/C of 1.7 produced a  
3 noticeable amount of CH<sub>4</sub> (up to 0.11 mol/mol-CH<sub>3</sub>OH). The effects of the Ni-Cu alloy phase in the  
4 reaction for all bimetallic catalysts were observed from the negligible amounts of CH<sub>4</sub> produced during  
5 the reaction, which means that the alloy phase is responsible for decreasing the hydrogenation effects of  
6 CO or CO<sub>2</sub> to produce CH<sub>4</sub>.

## 8 **3.2 Catalyst characterization**

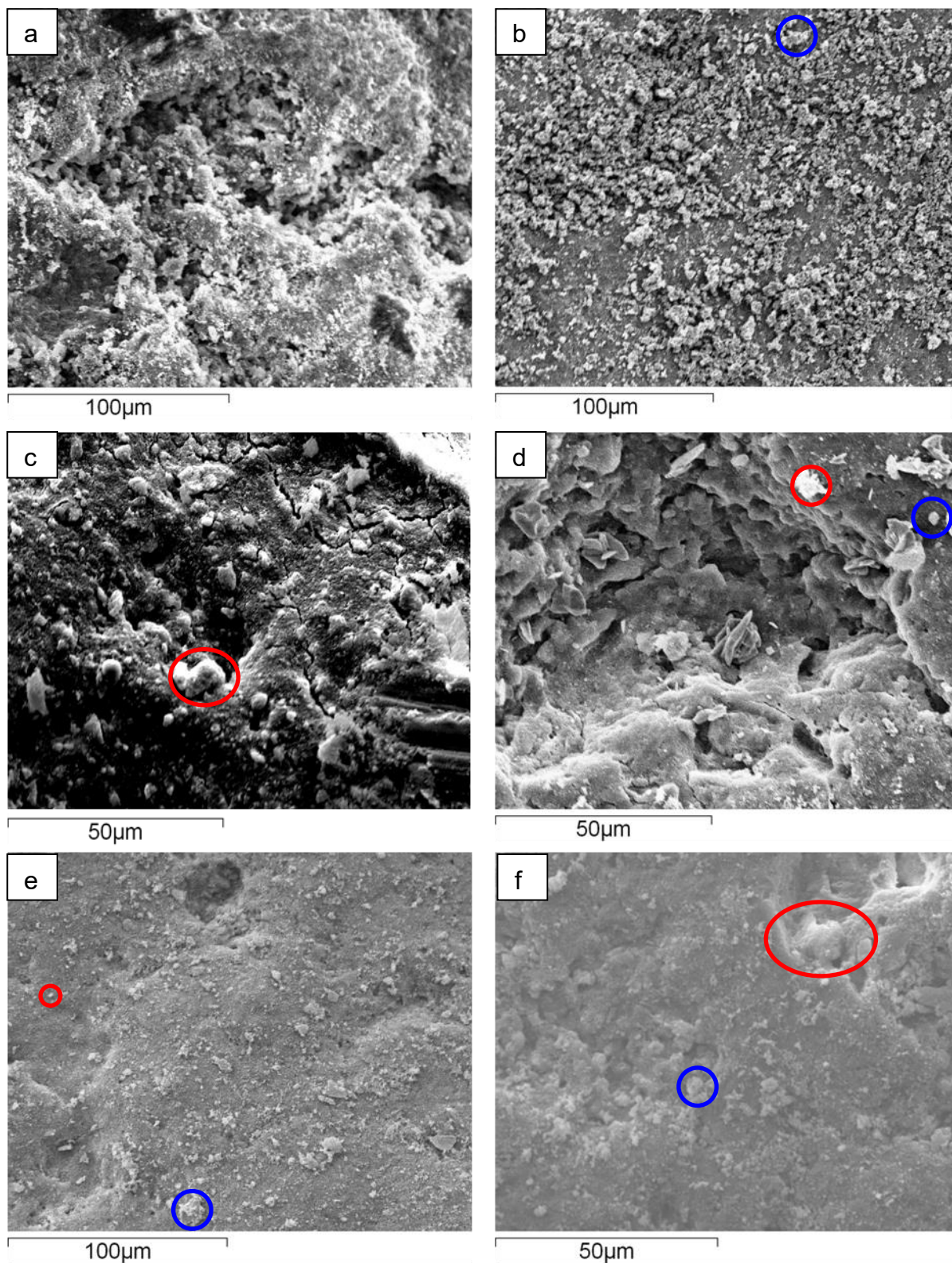
### 9 **3.2.1 SEM Imaging**

10 Fig.4 shows the SEM images for all the prepared catalysts. Fig. 4a presents the Al<sub>2</sub>O<sub>3</sub> support and the  
11 variation in darkness from light grey (low aluminium concentrations) to dark grey (high aluminium  
12 concentrations). Fig.4b presents the catalyst with 10% Cu and the copper species as shaded white patches  
13 (highlighted by a marked blue circle) distributed over a light grey background of Al<sub>2</sub>O<sub>3</sub> support. The  
14 estimated size of particles is 5-15 μm. The SEM image of 10%Ni/Al<sub>2</sub>O<sub>3</sub> catalyst in Fig.4c shows an  
15 irregular distribution of bright white spherical species (highlighted by a marked red circle) upon a dark  
16 grey background of Al<sub>2</sub>O<sub>3</sub> with particle size of 6-12 μm. Fig.4d shows the surface morphology of 7%Cu-  
17 3%Ni/Al<sub>2</sub>O<sub>3</sub> catalyst. Copper species (shaded white, highlighted by a marked blue circle) and Ni species  
18 (bright white, highlighted by a marked red circle), the approximate size of species is 6.5 μm. Performing  
19 SEM for 5%Cu-5%Ni shows that both Cu particles (shaded white, highlighted by a marked blue circle)  
20 and Ni particles (bright white, highlighted by a marked red circle) are distributed throughout the light  
21 grey of the Al<sub>2</sub>O<sub>3</sub> support with approximate sizes 4.4-10.9 μm. Agglomerates of larger particle sizes  
22 (highlighted by a marked red circle) are apparent in the 7%Ni-3%Cu sample (Figure 4f) compared to  
23 7%Cu-3%Ni (Figure 4d) and 5%Ni-5%Cu (Figure 4e) samples. Introducing additional Ni to the  
24 bimetallic system caused morphological changes compared to 7%Cu-3%Ni and 5%Ni-5%Cu samples  
25 [26]. This is related to the fact that Ni species normally reveal more agglomerates with increasing Ni  
26 concentration [27].

27

28

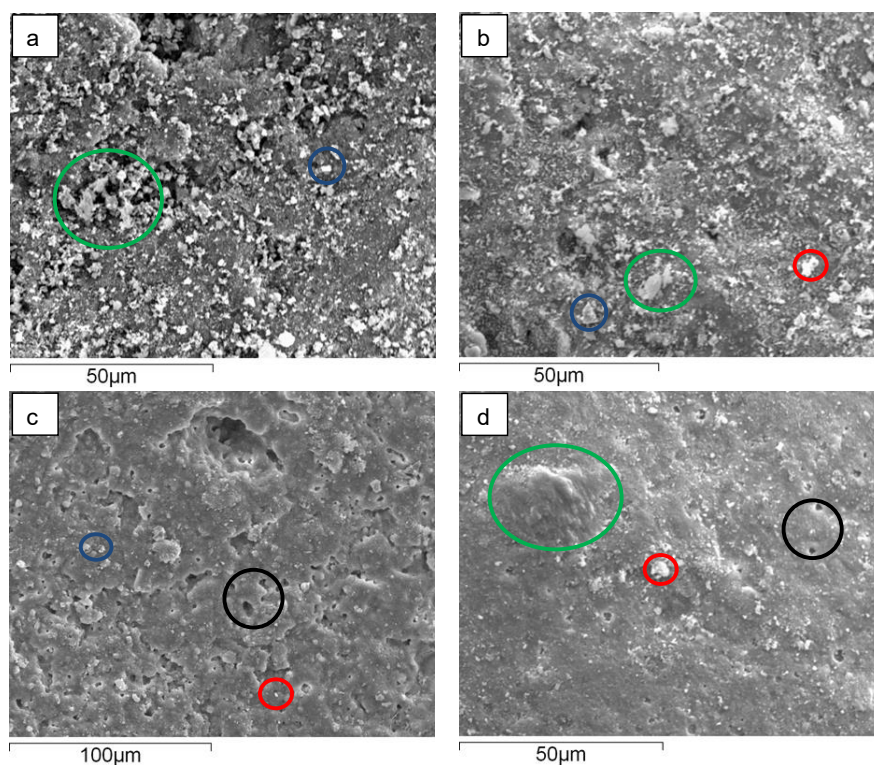




1  
 2 Fig.4. SEM images of the prepared catalysts: a)  $Al_2O_3$ , b) 10%Cu, c) 10%Ni, d) 7%Cu-3%Ni, e) 5%Cu-5%Ni and  
 3 f) 7%Ni-3%Cu.  
 4 The morphological appearance of the prepared catalysts post the reaction (10% Cu, 7% Cu-3%Ni, 5% Cu-  
 5 5%Ni and 3%Cu-7%Ni) operated at 225°C and 325°C and the S/C of 1.7 are shown in Figures 5 and 6,

1 respectively. The SEM images of the used 10%Cu catalyst which had been previously exposed to a  
2 temperature of 225°C during reaction, depicted in Figure 5a, shows a shade of white spots which  
3 correspond to Cu species (highlighted by a marked blue circle) distributed over grey Al<sub>2</sub>O<sub>3</sub> support. Small  
4 agglomerates of particles are apparent on the left side of the image (highlighted by a marked green circle).  
5 The distribution of particles showed uniformity over the support. The SEM image of the used 10%Cu  
6 catalyst reacted at 325°C in Figure 6a showed shade white spots (highlighted by a marked blue circle)  
7 which represent Cu species distributed over shades of grey Al<sub>2</sub>O<sub>3</sub> support but more agglomeration  
8 (highlighted by a marked green circle) have appeared on the catalyst compared to the SEM image of the  
9 used 10%Cu catalyst reacted at 225°C. This would be explained by the fact that increasing the reaction  
10 temperature to 325°C leads to the sintering of copper crystallites, causing coarsening [28].

11



12

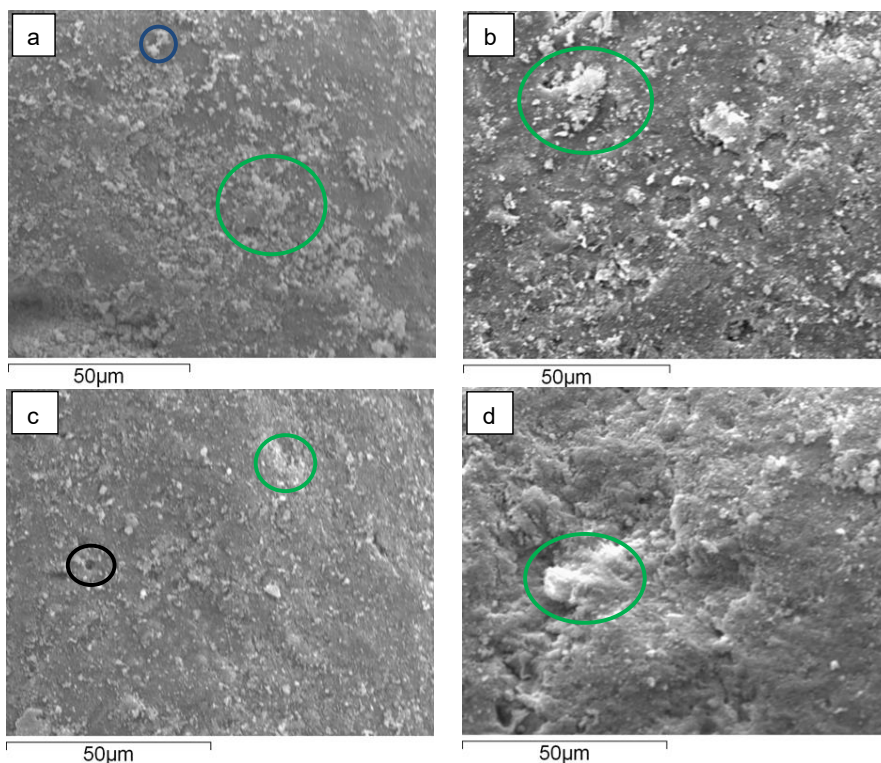
13

14 *Fig.5. SEM images of the used methanol catalysts reacted at 225°C and S/C of 1.7: a) 10%Cu, b) 7%Cu-3%Ni, c)*  
15 *5%Cu-5%Ni and d) 3%Cu-7%Ni.*

16

17





1

2 *Fig.6. SEM images of the used methanol catalysts reacted at 325°C and S/C of 1.7: a) 10%Cu, b) 7%Cu-3%Ni, c)*  
 3 *5%Cu-5%Ni and d) 3%Cu-7%Ni.*

4 The surface morphology of the used 7%Cu-3%Ni catalyst reacted at 225°C is showed in Figure 5b.  
 5 Shades of white spots which represent Cu species (highlighted by a marked blue circle) and bright white  
 6 spots which refer to Ni species (highlighted by a marked red circle) are distributed uniformly across the  
 7 surface of the aluminium support with small agglomerates of particles appearing on the catalyst surface  
 8 (highlighted by a marked green circle). Figure 6b shows the SEM image of the used catalyst operated at  
 9 325°C in the reaction, from which it is observed that larger agglomerates of particles appear on the  
 10 catalyst surface (highlighted by a marked green circle) compared to 7%Cu-3%Ni reacted at temperature  
 11 225°C.

12

13 The SEM image of the used 5%Cu-5%Ni reacted at 225°C in Figure 5c shows shades of white spots  
 14 which correspond to Cu species (highlighted by a marked blue circle) and bright white spots which  
 15 represent Ni species (highlighted by a marked red circle) distributed across the surface of the Al<sub>2</sub>O<sub>3</sub>  
 16 support. The SEM image of the used 5%Cu-5%Ni reacted at 325°C is reported in Fig.6c. It is observed  
 17 that a uniform distribution of species occurs with smaller agglomerates (highlighted by a marked green

1 circle) compared to the used 10%Cu and 7%Cu-3%Ni catalysts reacted at 325°C. However, some cracks  
2 (highlighted by a marked black circle) are visible for the used 5%Cu-5%Ni reacted at 225°C and 325°C.

3

4 The SEM image in Figure 5d for the used 3%Cu-7%Ni reacted at 225°C showed bright white spots which  
5 refer to Ni species (highlighted by a marked red circle) throughout the support with large agglomerates  
6 (highlighted by a marked green circle) and cracks observed on the surface (highlighted by a marked black  
7 circle). From Figure 6d, the used 3%Cu-7%Ni catalyst reacted at 325°C showed large agglomerates of  
8 bright white spots which correspond to Ni species agglomeration (highlighted by a marked green circle).

9

### 10 **3.2.2 BET surface area**

11 The BET surface area for fresh prepared catalyst showed that the surface area ranged from 120 m<sup>2</sup>/g for  
12 10%Cu to 128 m<sup>2</sup>/g for 5%Cu-5%Ni catalyst. The surface area of trilobe alumina used as support was  
13 142 m<sup>2</sup>/g. Impregnated samples resulted in a lower surface area with respect to pure Al<sub>2</sub>O<sub>3</sub> due to pore  
14 blockage during metal deposition. The BET surface area showed that the used catalysts had a lower  
15 surface area than the fresh catalysts as summarized in Table 2. This  
16 behaviour can be explained by the pore-blockage of the support after the reaction. Both temperatures  
17 showed similar results indicating that increasing the reaction temperature from 225°C to 325°C causes  
18 only minor changes to the catalyst surface area.

19

20 *Table 2. BET surface area for the fresh and used methanol catalysts reacted at 225°C, 325°C and S/C of 1.7.*

21

22

	Surface area (m <sup>2</sup> /g)		
	fresh	reacted at 225°C	reacted at 325°C
<b>10%Ni</b>	122	119	117
<b>10%Cu</b>	120	96	98
<b>7%Cu-3%Ni</b>	125	94	94
<b>5%Cu-5%Ni</b>	128	90	89
<b>3%Cu-7%Ni</b>	125	94	95

29

30

### 1 3.2.3 TPR

2 The hydrogen uptake for the catalyst reduction is shown in Fig.7. The 10%Cu catalyst is reduced at  
3 250°C. The wide peak at this reduction temperature is attributed to the dispersion of CuO over the Al<sub>2</sub>O<sub>3</sub>  
4 support and the amount of hydrogen required reacting with reducible particles. The finding agrees with  
5 that found by Jones and Hagelin [29]. The 10%Ni catalyst revealed multi broad peaks at 400°C and  
6 650°C. Both peaks are attributed to a range of interactions between NiO and the Al<sub>2</sub>O<sub>3</sub> support. The  
7 reduction temperature at 400°C corresponds to weak interaction between NiO and Al<sub>2</sub>O<sub>3</sub> support and the  
8 reduction temperature at 650°C is likely to be related to a strong interaction of NiO and Al<sub>2</sub>O<sub>3</sub>[30-32].  
9 The TPR profile of the bimetallic Ni-Cu catalysts (Fig. 7) shows three hydrogen uptake peaks. The first  
10 obtained peak on 7%Cu-3%Ni and 5%Cu-5%Ni showed high hydrogen uptake compared to 7%Ni-  
11 3%Cu. This indicates that a high area of hydrogen uptake peaks is related to the amount of reducible  
12 species of CuO, which increases in samples containing higher percentages of Cu. Therefore, the first  
13 sharp peak is associated with pure CuO and is shifted compared to the monotype Cu catalysts due to  
14 different amounts of Cu loadings and the rate of hydrogen uptake on CuO species. The broad peak in the  
15 middle (350°C for 7%Cu-3%Ni, 380°C for 5%Cu-5%Ni, 425°C for 7%Ni-3%Cu) of the TPR trace for  
16 the bimetallic catalyst can be associated with NiCuO interaction with support which was used to  
17 determine the reduction temperature for the subsequent reaction study. In addition, it can also indicate a  
18 weak interaction of NiO with support. The last peak is related to a strong interaction of NiO with the  
19 support. The difference in the position of reduction peaks reported here is related to the fact that the  
20 temperature of the reduction peaks strongly depend on the particle dimension and the interaction strength  
21 between metal particles and the support[15].

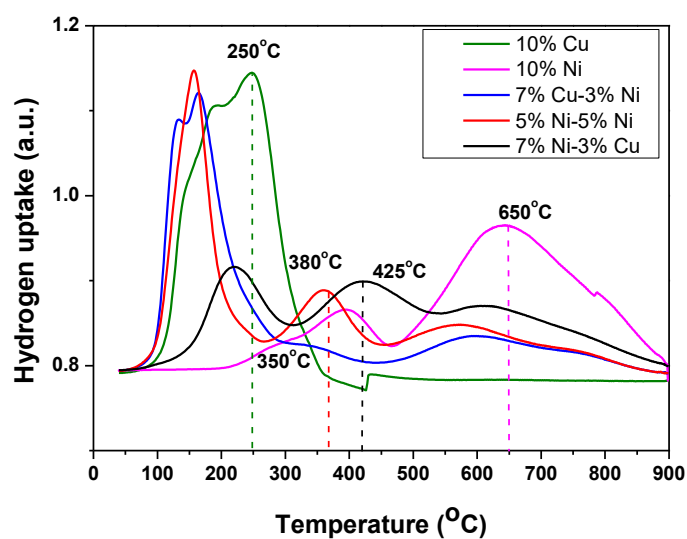


Fig.7. TPR for the prepared catalysts.

### 3.2.4 XRD

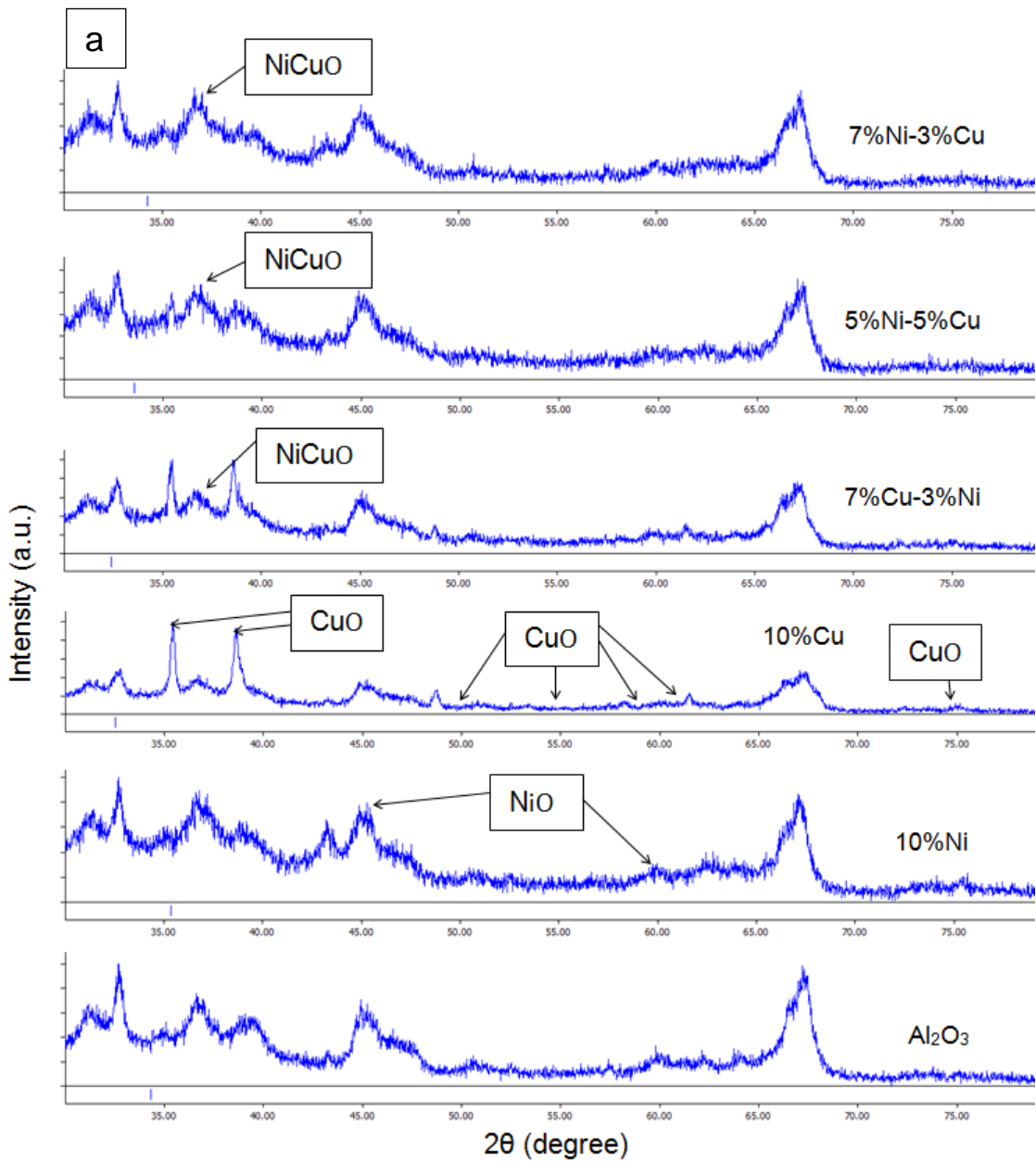
The XRD pattern performed for the unused catalyst is shown in Fig.8a. The monotype catalyst suggested the existence of NiO in the 10%Ni catalyst sample at ( $2\theta = 45^\circ, 60^\circ$ ) with the average crystallite diameter calculated by Scherrer's equation ( $L = \frac{K\lambda}{\beta \cos \theta}$ ) of 17.8 nm. The monotype catalyst of 10%Cu showed

XRD patterns of CuO spectra at ( $2\theta = 35^\circ, 39^\circ, 50^\circ, 55^\circ, 58^\circ, 61^\circ, 75^\circ$ ) and the average crystallite size of CuO was 17.9 nm. On the other hand, the bimetallic catalysts indicated the formation of NiO, CuO phases and  $Ni_xCu_{1-x}O$  phase at ( $2\theta = 36^\circ$ ). For instance, the crystallite diameter size of  $Ni_xCu_{1-x}O$  was 16.7 nm.

The XRD patterns for the used catalysts operated at 225°C and 325°C and S/C of 1.7 are shown in Fig.8b and Fig.8c, respectively. The XRD patterns showed that no metal oxide phase was detected, except for aluminates related to the support material. The monotype catalyst 10%Cu showed XRD patterns of Cu metals at  $2\theta = 44^\circ, 50^\circ$  and  $72^\circ$  and the average crystallite size of Cu was 18.1 nm. The bimetallic used catalysts showed patterns related to metallic Ni and metallic Cu and for Ni-Cu. The average crystallite size of bimetallic catalysts is 16.8 nm at  $2\theta = 37^\circ$ . The formation of a Ni-Cu alloy reported in the literature depends on the amount of Ni contents, indicating the Ni rich alloy or Cu rich alloy catalyst [20, 33]. The rich Ni alloy phase or rich Cu alloy phase determines the reaction paths. For instance, a dominant decomposition reaction occurred with 7%Ni-3%Cu over the metallic phase of Ni which was concluded from the high concentration of CO produced at 225-275°C. However, 7%Cu-3%Ni showed a dominant

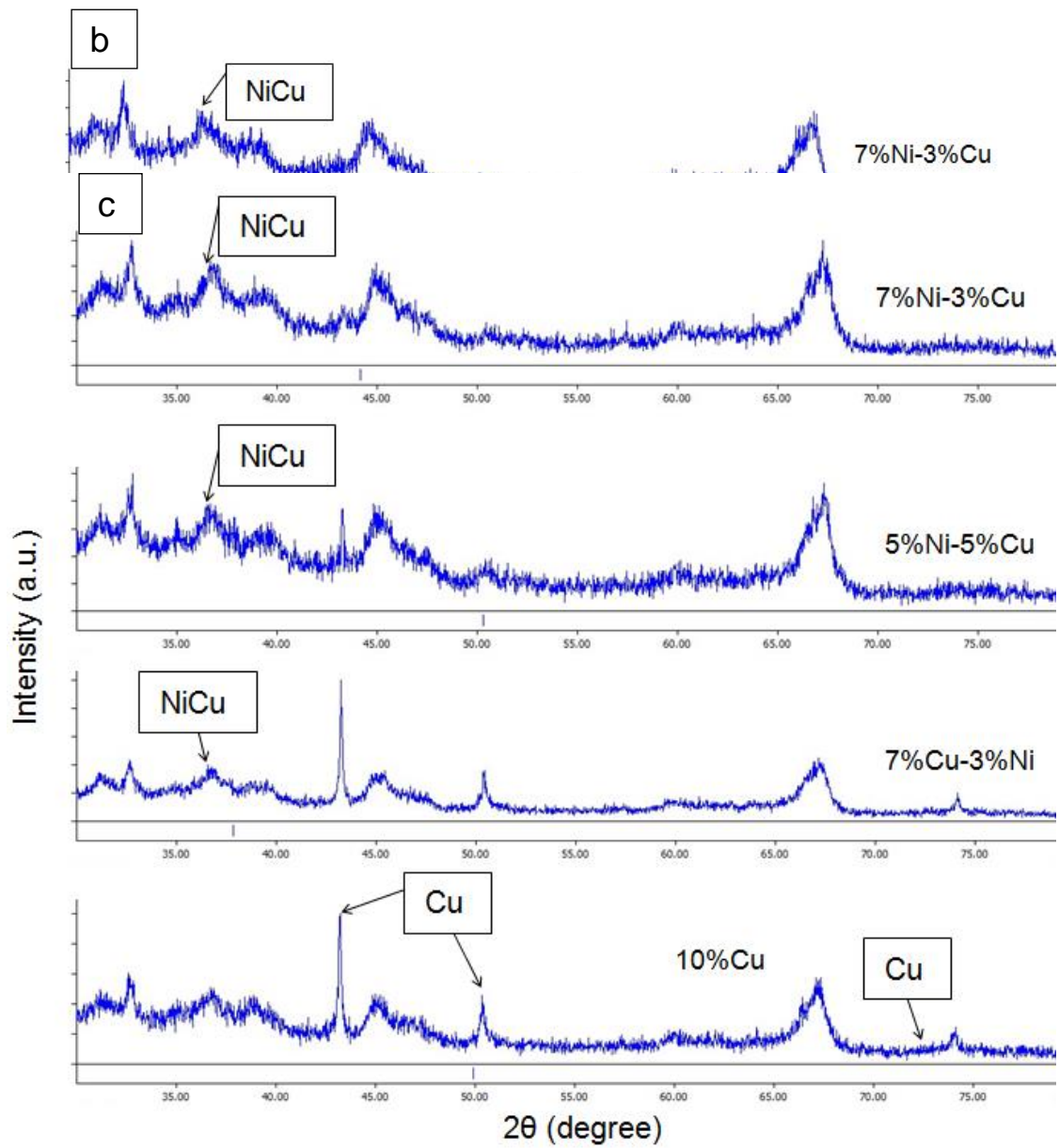
1 decomposition reaction over the metallic phase of Cu as a large amount of CO was produced at 300-  
2 325°C. The XRD patterns for used catalyst operated at 225°C and 325°C showed similar patterns, such  
3 that the effects of reaction temperature on the metal phase cannot be deduced. However, the XRD  
4 patterns displayed less diffuse and sharper patterns for the catalysts reacted at 325°C than 225°C. This  
5 would be possible due to crystallite growth with increasing the reaction temperature.

6  
7  
8  
9



10

1  
2  
3  
4  
5



6  
7

8 *Fig. 8.* XRD patterns for fresh and used catalysts: a) fresh catalysts, b) used catalysts reacted at 225°C and S/C of 1.7  
9 and c) used catalysts reacted at 325°C and S/C of 1.7.

10 **3.2.5 TGA**



1 Table 3 presents the results of carbon selectivity (Eq.4) for the reacted catalysts. The carbon formation  
 2 depends on the catalyst composition and reaction temperature [34]. The bimetallic rich Ni catalyst  
 3 (5%Cu-5%Ni and 3%Cu-7%Ni) reacted at temperature 300°C showed less carbon deposition than  
 4 10%Cu and 7%Cu-3%Ni. On other hand, 7%Cu-3%Ni and 3%Cu-7%Ni showed less carbon deposition  
 5 than 10%Cu reacted at temperature 250°C. The 10%Cu catalyst produced less carbon than 7%Cu-3%Ni  
 6 and 5%Cu-5%Ni reacted at temperature 225°C. It was found that the dominant reaction over Ni metals  
 7 is methanol decomposition reaction. Therefore, an abundance of CO was noticed in the reformat gases  
 8 with Ni containing catalysts compared to the gas composition from the 10%Cu catalyst. Previous work  
 9 in an alloying effects claimed that Cu surface energy is lower compared with Ni and a small size  
 10 mismatch between Cu and Ni allows Cu atoms to segregate on the Ni-Cu surface causing the Ni sites  
 11 responsible for carbon formation [35]. The Cu species doesn't easily dissociate CO at low temperature  
 12 [20, 36-38]. The current results of carbon formation can't deduce whether the Cu alloying with Ni has  
 13 any strong evidence that carbon selectivity can be reduced during methanol steam reforming for current  
 14 operation conditions.

15 *Table 3. Carbon selectivity on the used methanol catalysts reacted at 225-325°C and S/C of 1.7.*

16

	<b>10%Cu</b>	<b>7%Cu-3%Ni</b>	<b>5%Cu-5%Ni</b>	<b>3%Cu-7%Ni</b>
T (°C)	Sel <sub>C</sub> (%)	Sel <sub>C</sub> (%)	Sel <sub>C</sub> (%)	Sel <sub>C</sub> (%)
225	0.3	0.9	0.6	0.3
250	1.4	0.2	1.1	0.3
275	0.8	0.8	0.8	1.4
300	1.1	1.4	0.3	0.3
325	1.8	1.3	2.3	1.2

17

18

## 19 **4. Conclusions**

20 The increasing Ni metals content had a positive effect on methanol conversion and showed a high  
 21 methanol conversion at 300-325°C. The methanol conversion was high for 5%Cu-5%Ni and 7%Cu-  
 22 3%Ni (98.5%) at 325°C which could possibly be explained by the active decomposition reaction. The  
 23 current work also revealed that bimetallic catalytic performance affected the reformat compositions  
 24 compared to the monometallic catalysts trying to investigate if the metallic and alloy phase of metals will  
 25 affect the catalytic performance toward the syngas production in methanol steam reforming process. The  
 26 influence of increase the Ni content had shown an increase in CO and decrease in CO<sub>2</sub> yields. This

1 confirmed that Ni rich catalysts (more than 5wt%) is favourable for methanol decomposition reaction.  
2 The bimetallic catalyst did not produce any CH<sub>4</sub>, revealing that Cu alloying in Ni catalyst had an  
3 inhibiting effect for CO and/or CO<sub>2</sub> hydrogenation. The results showed that Cu-based catalysts had good  
4 activity for the water gas shift reaction, and had no methanation activity. The existence of single Ni  
5 catalyst in the reactor promoted CH<sub>4</sub> formation by CO and CO<sub>2</sub> hydrogenation. The reaction over physical  
6 mixture of catalyst showed less CO and more CO<sub>2</sub> than the bimetallic catalytic system. This indicated  
7 that the 10 wt % Cu catalyst in the physical mixture of catalyst controls the high activity of the water gas  
8 shift reaction. The current results of carbon formation can't deduce whether the Cu alloying with Ni has  
9 any strong evidence that carbon selectivity can be reduced during methanol steam reforming for current  
10 operation conditions.

## 11 **References:**

- 12 [1] Little A. Multi-fuel reformers for fuel cells used in transportation. Phase 1: Multi-fuel reformers.  
13 Cambridge 1994.  
14 [2] Sofoklis SM. Hydrogen storage and compression: Institution of Engineering and Technology.  
15 [3] Gkanas EI, Khzouz M, Panagakos G, Statheros T, Mihalakakou G, Siasos GI, et al. Hydrogenation  
16 behavior in rectangular metal hydride tanks under effective heat management processes for green  
17 building applications. *Energy*. 142:518-30.  
18 [4] Lwin Y, Daud WRW, Mohamad AB, Yaakob Z. Hydrogen production from steam-methanol  
19 reforming: Thermodynamic analysis. *International Journal of Hydrogen Energy*. 2000;25:47-53.  
20 [5] Kolb G. Fuel Processing For Fuel Cells. Weinheim: Wiley-VCH; 2008.  
21 [6] Peppley BA, Amphlett JC, Kearns LM, Mann RF. Methanol-steam reforming on Cu/ZnO/Al<sub>2</sub>O<sub>3</sub>  
22 catalysts. Part 2. A comprehensive kinetic model. *Applied Catalysis A: General*. 1999;179:31-49.  
23 [7] Peppley BA, Amphlett JC, Kearns LM, Mann RF. Methanol-steam reforming on Cu/ZnO/Al<sub>2</sub>O<sub>3</sub>. Part  
24 1: the reaction network. *Applied Catalysis A: General*. 1999;179:21-9.  
25 [8] Agarwal V, Patel S, Pant KK. H<sub>2</sub> production by steam reforming of methanol over Cu/ZnO/Al<sub>2</sub>O<sub>3</sub>  
26 catalysts: transient deactivation kinetics modeling. *Applied Catalysis A: General*. 2005;279:155-64.  
27 [9] Purnama H, Ressler T, Jentoft RE, Soerijanto H, Schlögl R, Schomäcker R. CO formation/selectivity  
28 for steam reforming of methanol with a commercial CuO/ZnO/Al<sub>2</sub>O<sub>3</sub> catalyst. *Applied Catalysis A:  
29 General*. 2004;259:83-94.  
30 [10] Basile A, Parmaliana A, Tosti S, Iulianelli A, Gallucci F, Espro C, et al. Hydrogen production by  
31 methanol steam reforming carried out in membrane reactor on Cu/Zn/Mg-based catalyst. *Catalysis  
32 Today*. 2008;137:17-22.  
33 [11] Amphlett JC, Creber KAM, Davis JM, Mann RF, Peppley BA, Stokes DM. Hydrogen production  
34 by steam reforming of methanol for polymer electrolyte fuel cells. *International Journal of Hydrogen  
35 Energy*. 1994;19:131-7.  
36 [12] Peters R, Düsterwald HG, Höhle B. Investigation of a methanol reformer concept considering the  
37 particular impact of dynamics and long-term stability for use in a fuel-cell-powered passenger car.  
38 *Journal of Power Sources*. 2000;86:507-14.  
39 [13] Wu H, La Parola V, Pantaleo G, Puleo F, Venezia A, Liotta L. Ni-Based Catalysts for Low  
40 Temperature Methane Steam Reforming: Recent Results on Ni-Au and Comparison with Other Bi-  
41 Metallic Systems. *Catalysts*. 2013;3:563-83.  
42 [14] Angeli SD, Monteleone G, Giaconia A, Lemonidou AA. State of the art catalysts for CH<sub>4</sub> steam  
43 reforming at low temperature. *International Journal of Hydrogen Energy*. 2014;39:1979-97.  
44 [15] Khzouz M, Wood J, Kendall K, Bujalski W. Characterization of Ni-Cu-based catalysts for multi-  
45 fuel steam reformer. *International Journal of Low-Carbon Technologies*. 2012;7:55-9.

- 1 [16] Carrero A, Calles JA, Vizcaíno AJ. Hydrogen production by ethanol steam reforming over Cu-  
2 Ni/SBA-15 supported catalysts prepared by direct synthesis and impregnation. *Applied Catalysis A:*  
3 *General*. 2007;327:82-94.
- 4 [17] Vizcaíno AJ, Carrero A, Calles JA. Hydrogen production by ethanol steam reforming over Cu-Ni  
5 supported catalysts. *International Journal of Hydrogen Energy*. 2007;32:1450-61.
- 6 [18] Mariño F, Boveri M, Baronetti G, Laborde M. Hydrogen production from steam reforming of  
7 bioethanol using Cu/Ni/K/ $\gamma$ -Al<sub>2</sub>O<sub>3</sub> catalysts. Effect of Ni. *International Journal of Hydrogen Energy*.  
8 2001;26:665-8.
- 9 [19] Liao P-H, Yang H-M. Preparation of catalyst Ni-Cu/CNTs by chemical reduction with  
10 formaldehyde for steam reforming of methanol. *Catalysis Letters*. 2008;121:274-82.
- 11 [20] De Rogatis L, Montini T, Lorenzut B, Fornasiero P. Ni<sub>x</sub>Cu<sub>y</sub>/Al<sub>2</sub>O<sub>3</sub> based catalysts for hydrogen  
12 production. *Energy & Environmental Science*. 2008;1:501-9.
- 13 [21] Khzouz M, Wood J, Pollet B, Bujalski W. Characterization and activity test of commercial Ni/Al<sub>2</sub>O<sub>3</sub>,  
14 Cu/ZnO/Al<sub>2</sub>O<sub>3</sub> and prepared Ni-Cu/Al<sub>2</sub>O<sub>3</sub> catalysts for hydrogen production from methane and methanol  
15 fuels. *International Journal of Hydrogen Energy*. 2013;38:1664-75.
- 16 [22] Brunauer S, Emmett PH, Teller E. Adsorption of gases in multimolecular layers. Contribution from  
17 the bureau of chemistry and soils and george washington university. 1938.
- 18 [23] Khzouz M, Gkanas E. Experimental and Numerical Study of Low Temperature Methane Steam  
19 Reforming for Hydrogen Production. *Catalysts*.8:5.
- 20 [24] NETZSCH. Operating instructions TG 209 F1 iris. Gemany: NETZSCH-Gerätebau GmbH.
- 21 [25] Post E. Principles of TG, DSC, STA and EGA. Germany: NETZSCH; 2009.
- 22 [26] Echegoyen Y, Suelves I, Lázaro MJ, Sanjuán ML, Moliner R. Thermo catalytic decomposition of  
23 methane over Ni-Mg and Ni-Cu-Mg catalysts: Effect of catalyst preparation method. *Applied Catalysis*  
24 *A: General*. 2007;333:229-37.
- 25 [27] Lázaro MJ, Echegoyen Y, Suelves I, Palacios JM, Moliner R. Decomposition of methane over Ni-  
26 SiO<sub>2</sub> and Ni-Cu-SiO<sub>2</sub> catalysts: Effect of catalyst preparation method. *Applied Catalysis A: General*.  
27 2007;329:22-9.
- 28 [28] Twigg MV, Spencer MS. Deactivation of copper metal catalysts for methanol decomposition,  
29 methanol steam reforming and methanol synthesis. *Topics in Catalysis*. 2003;22:191-203.
- 30 [29] Jones SD, Hagelin-Weaver HE. Steam reforming of methanol over CeO<sub>2</sub>- and ZrO<sub>2</sub>-promoted Cu-  
31 ZnO catalysts supported on nanoparticle Al<sub>2</sub>O<sub>3</sub>. *Applied Catalysis B: Environmental*. 2009;90:195-204.
- 32 [30] De Rogatis L, Montini T, Cognigni A, Olivi L, Fornasiero P. Methane partial oxidation on NiCu-  
33 based catalysts. *Catalysis Today*. 2009;145:176-85.
- 34 [31] Roh H-S, Jun K-W, Dong W-S, Chang J-S, Park S-E, Joe Y-I. Highly active and stable Ni/Ce-ZrO<sub>2</sub>  
35 catalyst for H<sub>2</sub> production from methane. *Journal of Molecular Catalysis A: Chemical*. 2002;181:137-  
36 42.
- 37 [32] Ye J, Li Z, Duan H, Liu Y. Lanthanum modified Ni/ $\gamma$ -Al<sub>2</sub>O<sub>3</sub> catalysts for partial oxidation of  
38 methane. *Journal of Rare Earths*. 2006;24:302-8.
- 39 [33] Lee J-H, Lee E-G, Joo O-S, Jung K-D. Stabilization of Ni/Al<sub>2</sub>O<sub>3</sub> catalyst by Cu addition for CO<sub>2</sub>  
40 reforming of methane. *Applied Catalysis A: General*. 2004;269:1-6.
- 41 [34] Bartholomew CH. Mechanisms of catalyst deactivation. *Applied Catalysis A: General*.  
42 2001;212:17-60.
- 43 [35] Ferrando R, Jellinek J, Johnston RL. Nanoalloys: From theory to applications of alloy clusters and  
44 nanoparticles. *Chemical Reviews*. 2008;108:845-910.
- 45 [36] Ponec V. Selectivity in the syngas reactions: The role of supports and promoters in the activation of  
46 CO and in the stabilization of intermediates: Elsevier; 1991.
- 47 [37] Schwank J. Bimetallic catalysts for CO activation. *Studies in Surface Science and Catalysis*:  
48 Elsevier; 1991. p. 225-64.
- 49 [38] Ponec V, Bond GC. *Catalysis by metals and alloys*: Elsevier; 1995.

50  
51